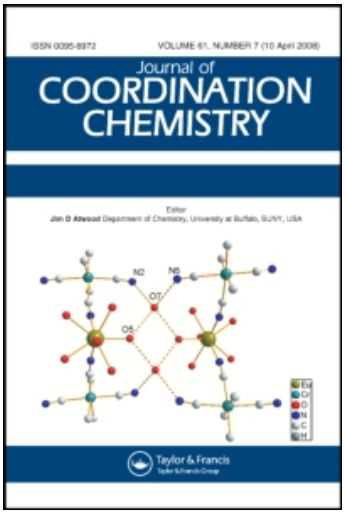

Journal of Coordination Chemistry
Publication details, including instructions for authors and subscription information:
http://www.informaworld.com/smpp/title~content=t713455674

Synthesis, structure, and electrochemistry of *mer*[$RuCl_3$(DMSO-S)(DMSO-O)(py)]

Radhey S. Srivastava[a]; Frank R. Fronczek[b]; Richard S. Perkins[a]
[a] Department of Chemistry, University of Louisiana at Lafayette, Lafayette, LA 70504, USA [b] Department of Chemistry, Louisiana State University, Baton Rouge, LA 70803, USA

To cite this Article Srivastava, Radhey S. , Fronczek, Frank R. and Perkins, Richard S.(2009) 'Synthesis, structure, and electrochemistry of *mer*[$RuCl_3$(DMSO-S)(DMSO-O)(py)]', Journal of Coordination Chemistry, 62: 23, 3745 — 3753
To link to this Article: DOI: 10.1080/00958970903193981
URL: http://dx.doi.org/10.1080/00958970903193981

Journal of Coordination Chemistry
Vol. 62, No. 23, 10 December 2009, 3745–3753

Taylor & Francis
Taylor & Francis Group

Synthesis, structure, and electrochemistry of *mer*-[$RuCl_3$(DMSO–S)(DMSO–O)(py)]

RADHEY S. SRIVASTAVA*†, FRANK R. FRONCZEK‡ and RICHARD S. PERKINS†

†Department of Chemistry, University of Louisiana at Lafayette, Lafayette, LA 70504, USA
‡Department of Chemistry, Louisiana State University, Baton Rouge, LA 70803, USA

(*Received 5 January 2009; in final form 23 March 2009*)

Reaction of *mer*-[$RuCl_3$(DMSO–S)$_2$(DMSO–O] (**1**) with pyridine (py) in dichloromethane yields *mer*-[$RuCl_3$(DMSO–S)(DMSO–O)(py)] (**2**). A single crystal suitable for X-ray diffraction was obtained by recrystalization with dichloromethane and diethyl ether. X-ray diffraction analysis revealed an unusual case in which two independent molecules (**2a** and **2b**) are present in the asymmetric unit cell. Both molecules have distorted octahedral geometry in which DMSO is bound through oxygen and sulfur. Density functional theory (DFT) calculations were performed for **2a** and **2b** in gas phase to investigate bonding shown by the two DMSO ligands. Optimizations were done on both DMSO ligands bonded through S, both DMSO ligands bonded through O, one DMSO bonded through O, and the other through S but opposite to the actual molecule. The energy differences of the optimized structures were calculated.

Keywords: Ruthenium complexes; X-ray structure; Meridonial (*mer*); Electrochemistry; DMSO

1. Introduction

Ruthenium complexes attract a great deal of attention due to their applications as catalysts for different processes including redox reactions [1], molecular machine-type devices [2], molecular switching devices [3], and molecular memories [4] because of the ability of the Ru–DMSO bond to undergo linkage isomerism.

In bioinorganic chemistry, ruthenium complexes are utilized as probes for understanding electron-transfer processes and oxidations in DNA [5]. Ruthenium (II, III) complexes also display anticancer activity and antimetastatic properties [6, 7]; some of these complexes are under intensive clinical investigation [8].

Ruthenium and platinum complexes with *N*-heterocyclic ligands show significant toxicity [9]. Ruthenium–pyridine complexes belong to a series of structurally similar complexes of the type *mer*-[$RuCl_3$(DMSO–S)(DMSO–O)(N)] in which only the nature of the nitrogen ligand was changed. The synthesis of **2** was earlier claimed by Alessio *et al.* [10] on the basis of spectroscopy; however, no X-ray structure was reported. However, we found that the reported complex is an unusual example, where two

*Corresponding author. Email: rss1805@louisiana.edu

ISSN 0095-8972 print/ISSN 1029-0389 online © 2009 Taylor & Francis
DOI: 10.1080/00958970903193981

independent molecules are present in the asymmetric unit cell. We report here the synthesis and unequivocal characterization of *mer*-[$RuCl_3$(DMSO–S)(DMSO–O)(py)] complex.

2. Experimental

All reagents were of analytical grade. The solvents employed were of reagent grade and dried over 4 Å molecular sieves. Pyridine was distilled before use. IR spectra were measured on a JASCO 480 Plus spectrophotometer with samples in KBr discs. UV-Vis spectra were obtained on a JASCO V-550 spectrophotometer. Elemental analysis was performed by Atlantic Microlab, Norcross, Georgia. [$H(DMSO)_2$][*trans*-$RuCl_4(DMSO)_2$] and *mer*-[$RuCl_3$(DMSO–S)$_2$(DMSO–O)] **1** were prepared according to the literature procedures [11]. A cyclic voltammetry (in DMSO) arrangement was used as described previously [12]. Argon was bubbled through the solution for at least 30 min prior to cyclic voltammetry and passed above the solution during cyclic voltammetry. Instrumental iR compensation was used when needed. In some experiments the electrode was rotated. The concentration of **2** was 1.00 mM.

2.1. *X-ray structure determination*

Diffraction data were collected at low temperature on a Nonius KappaCCD diffractometer equipped with Mo-Kα radiation ($\lambda = 0.71073$ Å), a graphite monochromator, and an Oxford Cryostream low-temperature device. Absorption corrections were carried out by the multi-scan method. Hydrogen atoms were visible in difference maps, but were placed in calculated positions for refinement, and a torsional parameter was refined for each methyl group. Crystal data and details of data collection and refinement are given in table 1.

2.2. *Computational studies*

Density functional theory (DFT) computations were carried out using Gaussian03 [13].

2.3. *Synthesis of* mer-*[$RuCl_3$(DMSO-S)(DMSO-O)(py)]*

A 0.05 g (0.34 mmol) sample of pyridine and 0.146 g (0.32 mmol) of *mer*-[$RuCl_3$(DMSO–S)$_2$)DMSO–O)] were dissolved in 20 mL of dichloromethane and refluxed for 24 h. Solvent was removed under reduced pressure, and then triturated with diethyl ether to get yellow-orange solid. The product was recrystalized in dichloromethane and hexane to obtain orange crystalline product suitable for X-ray diffraction. The product was filtered, washed with chilled dichloromethane and diethyl ether, and vacuum dried. The yield was 0.086 g (65%). Anal. Calcd for $C_9H_{17}Cl_3NO_2RuS_2$ (%) (MM = 442.78): C, 24.41; H, 3.87; N, 3.12. Found (%): C, 24.65; H, 3.96; N, 3.03. Selected IR absorption bands in KBr (cm^{-1}): ν_{SO} 1109 and 1020 (S–DMSO), ν_{SO} 913 (O–DMSO), ν 494 (Ru–O), ν 429 (Ru–N). UV-Vis (acetone): 435 nm ($\varepsilon = 290\ L\ mol^{-1}\ m^{-1}$); 375 nm ($\varepsilon = 829\ L\ mol^{-1}\ m^{-1}$).

Table 1. Crystal data for **2**.

CCDC deposit No.	CCDC 697452
Empirical formula	$C_9H_{17}Cl_3NO_2RuS_2$
Formula weight	442.78
Crystal	Orange lath
Crystal size (mm^3)	$0.05 \times 0.10 \times 0.23$
Crystal system	Monoclinic
Space group	$P2_1/c$
Temperature (K)	90
Unit cell dimensions (Å,°)	
a	11.9317(14)
b	16.2550(16)
c	16.412(2)
β	90.053(6)
Volume ($Å^3$), Z	3183.1(6), 8
Limiting indices	$-16 \le h \le +16$, $-20 \le k \le -22$, $-23 \le l \le +23$
θ range for data collection (°)	2.7–30.5
Absorption coefficient (mm^{-1})	1.74
Max. and min. transmission	0.690 and 0.918
Calculated density ($g\,cm^{-3}$)	1.848
Data collected	55,320
Observed/unique data	6100/8957
R	0.038
wR (F^2)	0.078
Parameters	334
Largest difference peak and hole ($e\,Å^{-3}$)	1.28 and −1.30

3. Results and discussion

3.1. *Synthesis and structure*

Equimolecular amounts of *mer*-[$RuCl_3$(DMSO–S)$_2$(DMSO–O)] (**1**) and pyridine were refluxed to produce *mer*-[$RuCl_3$(DMSO–S)(DMSO–O)(py)] (**2**) in good yield.

$$\left\{\begin{array}{c} \textit{mer}\text{-}[RuCl_3(DMSO{-}S)_2(DMSO{-}O)] \\ +\,\text{pyridine(py)} \end{array}\right\} \longrightarrow \textit{mer}\text{-}[RuCl_3(DMSO{-}S)(DMSO{-}O)(py)]$$

1 **2**

3.2. *X-ray crystal structure*

Compound **2** crystallized as monoclinic, space group $P2_1/c$ with two independent molecules (**2a** and **2b**) in the asymmetric unit cell, shown in figure 1. Ruthenium(III) is surrounded by (figure 1, table 1) six donors, S of one DMSO and O of another DMSO, one nitrogen of pyridine and three meridonial chloro ligands in a distorted octahedral coordination sphere. The pyridine is *trans* to the S-bound DMSO.

The Ru–S bond distances, 2.2736(9) and 2.2772(8) Å (table 2), are appreciably shorter than the average value of 2.34(1) Å found for Ru(III)–S *trans* to DMSO–S in the precursor [11, 14] and slightly shorter in the TMSO analog, *mer*-[$RuCl_3$(TMSO)(bpy)] 2.2969(8) [15]. The average Ru–Cl bond length, 2.3414(5) Å, is comparable to the NH_3 analog [10] and other related Ru(III) complexes [10, 16]. However, the Ru–Cl bond lengths *trans* to DMSO oxygen, 2.3247(8) and 2.3274(8) Å, are shorter than the other Ru–Cl distances, which fall in the range 2.3441(8)–2.3582(8) Å.

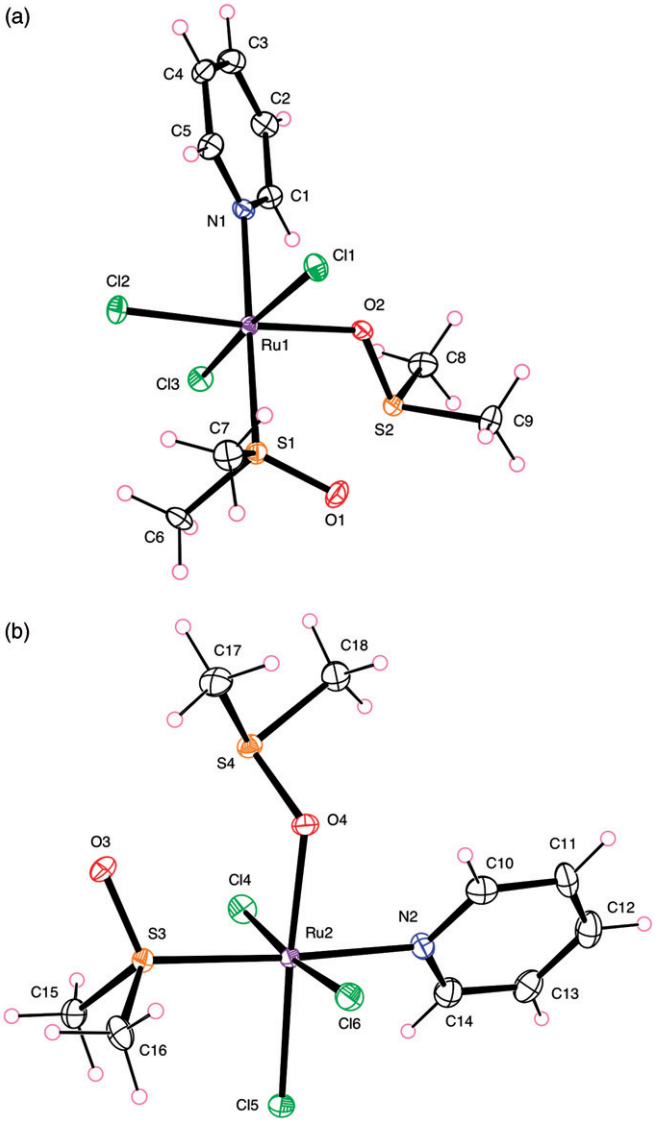

Figure 1. Structures of (a) *mer*-[$RuCl_3$(DMSO–S)(DMSO–O)(py)] (**2a**) and (b) *mer*-[$RuCl_3$(DMSO–S)(DMSO-O)(py)] (**2b**).

The Ru–DMSO–O (*trans* to Cl), Ru–pyridine nitrogen, and Ru–DMSO–S bond lengths are very close to *mer*-[$RuCl_3$(DMSO–S)(DMSO–O)(NH_3)] [10]. However, DMSO–S bond length in **2** and its NH_3 analog are shorter than its precursor due to increased back-bonding contribution from Ru(III). The O–Ru–N and S–Ru–O bond angles are smaller than *mer*-[$RuCl_3$(DMSO–S)(DMSO–O)(NH_3)].

The bond angles of N1Ru1S, 178.961(7)°; O2Ru1Cl, 175.64(6)°; and Cl1Ru1Cl3 173.26(3)° are slightly smaller than for octahedral. The bond angles of **2a** and **2b** are distinctly different from each other. For example, the bond angles S1Ru1N1 178.96(7)°

Table 2. Selected bond lengths (Å) and angles (°) for **2a** and **2b**.

	2a		**2b**
Bond angles			
Ru1–O2	2.062(2)	Ru2–O4	2.0674(19)
Ru1–N1	2.123(2)	Ru2–N2	2.127(3)
Ru–S1	2.2772(8)	Ru2–S3	2.2736(9)
Ru1–Cl2	2.3247(8)	Ru2–Cl5	2.3274(8)
Ru1–Cl1	2.3492(8)	Ru2–Cl4	2.3441(8)
Ru1–Cl3	2.3504(8)	Ru2–Cl6	2.3582(8)
Bond angles			
O2–Ru1–N1	84.96(9)	O4–Ru2–N2	85.36(9)
O2–Ru1–S1	95.08(6)	O4–Ru2–S3	91.59(6)
N1–Ru1–S1	178.96(7)	N2–Ru2–S3	176.23(7)
O2–Ru1–Cl2	175.64(6)	O4–Ru2–Cl5	176.47(6)
N1–Ru1–Cl2	90.69(7)	N2–Ru2–Cl5	92.37(7)
S1–Ru1–Cl2	89.28(3)	S3–Ru2–Cl5	90.77(3)
O2–Ru–Cl1	85.86(6)	O4–Ru2–Cl4	89.91(6)
N1–Ru1–Cl1	89.05(7)	N2–Ru2–Cl4	88.79(7)
S1–Ru1–Cl1	89.92(3)	S3–Ru2–Cl4	88.99(3)
Cl2–Ru1–Cl1	94.13(3)	Cl5–Ru2–Cl4	92.75(3)
O2–Ru1–Cl3	87.46(6)	O4–Ru2–Cl6	85.17(6)
N1–Ru1–Cl3	89.42(7)	N2–Ru2–Cl6	88.64(7)
S1–Ru1–Cl3	91.61(3)	S2–Ru2–Cl6	93.33(3)
Cl2–Ru1–Cl3	92.46(3)	Cl5–Ru2–Cl6	92.07(3)
Cl1–Ru1–Cl3	173.26(3)	Cl4–Ru2–Cl6	174.62(3)

and O2Ru1S1 95.08(6)° of **2a** are larger than S3Ru2N2, 176.23(7)° and O4Ru2S3 91.59(6)° of **2b**. The conformations of the two independent molecules differ mainly with respect to the O-bonded DMSO. Relative to the $RuCl_3$ units, the S-bonded DMSO ligands of the two molecules differ by a torsional difference of only 6.4° about the Ru–S bond. Similarly, the pyridine conformations differ by a twist of only 9.6° about Ru–N. However, the O-bonded DMSO ligand conformations differ by a 76.6° torsional twist about Ru–O.

3.3. *DFT calculation*

DFT calculations were carried out using Gaussian 03 [13]. The DFT method used was B3PW91 with a LANL2DZ basis set. Energy calculations were made for both the isomers of **2** as they appear in the crystal. These separate isomer structures differ in calculated energy by 12.4 kJ mol^{-1}. The structures **2a** and **2b** were also used as starting structures for the structure optimization of isolated molecules in the gas phase. Each gave a slightly different optimized structure. The two optimized structures differed in energy by 4.1 kJ mol^{-1}. Obtaining two structures illustrates the problem of optimizing to a local minimum. There may be many points of potential energy that are lower than the immediately surrounding points, but only one of these points is the global minimum. For a complicated molecule, it is difficult to obtain a global minimum with certainly using a small number of calculations. The two optimized structures obtained above differ mostly in the rotation around a bond in a DMSO ligand. The more stable of the two structures will be used for comparisons with the calculations described below.

The different bonding shown by the two DMSO ligands (one through S and the other through O) was investigated somewhat by DFT gas phase optimizations of these bonding schemes with both DMSO ligands bonded through S, both DMSO ligands bonded through O, one DMSO bonded through O, and the other through S but opposite to the actual molecule (figure 2a–d).

Two optimizations were done with different starting structures with both DMSO ligands bonded through S. The energy of the two calculations differed only by 0.0035 kJ mol^{-1}. The structure obtained is less stable than the actual bonding optimized above. The difference in energy in the two types of bonding is 83.7 kJ mol^{-1}.

Two optimizations were done with bonding through S and O but opposite to the actual bonding. Two optimizations gave nearly the same structure with an energy difference of only 0.0040 kJ mol^{-1}. This structure was also less stable than the actual structure. The energy difference was 28.4 kJ mol^{-1}.

Two optimizations done with both DMSO ligands bonded through O gave a more stable structure than the actual structure. Two minima were obtained that differed in energy by 5.8 kJ mol^{-1}. Again, we have the above-mentioned problem of optimizing to a local minimum. As said above, we will use the lower of these two energies and compare this with the actual structure. When that is done, a difference of 24.4 kJ mol^{-1} is found. Why this bonding scheme is not what is experimentally realized may be due to solvent effects during synthesis and/or crystallization.

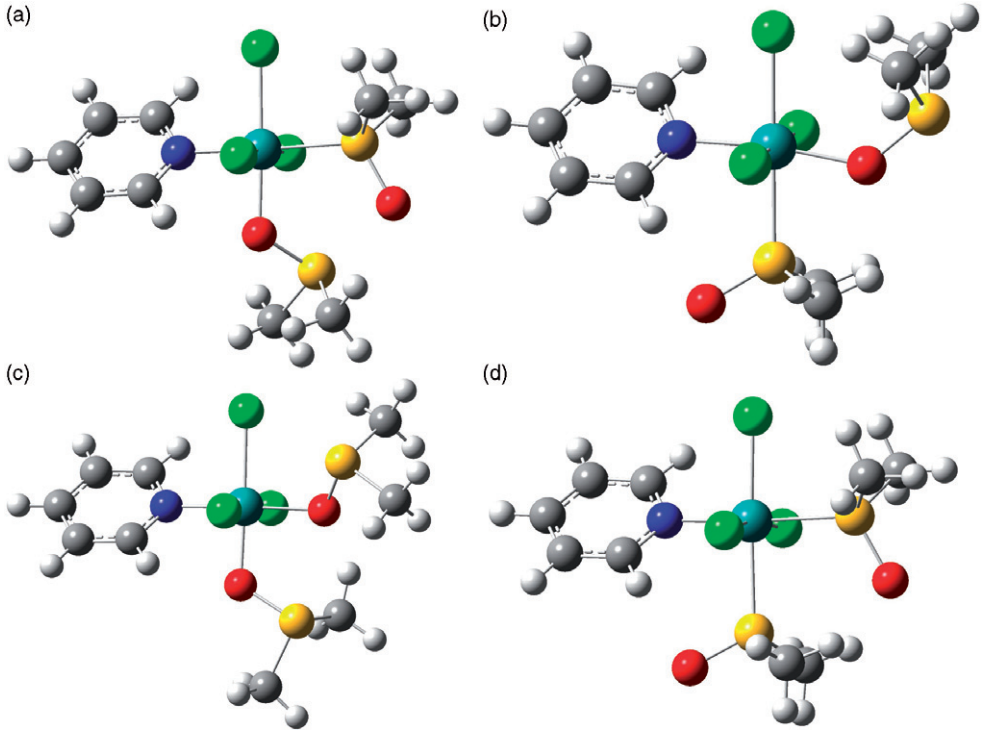

Figure 2. Optimized structure of *mer*-[$RuCl_3$(DMSO–S)(DMSO–O)(py)] **2** in gas phase in which (a) one DMSO is sulfur bonded and another via oxygen as in actual molecule in the crystal to ruthenium(III); (b) sulfur and oxygen bonded to ruthenium(III) is switched to figure 3(a); (c) both DMSO are oxygen bonded to ruthenium(III); and (d) both DMSO are sulfur bonded to ruthenium(III).

3.4. *Electrochemistry*

Cyclic voltammetry was carried out for **2** in DMSO at sweep rates ranging from 100 to 5120 mV s^{-1}. Figure 3 shows the resulting graph of the first reduction sweep followed by an oxidation sweep and another reduction sweep at a sweep rate of 200 mV s^{-1}. The ends of the sweeps correspond to the reduction and oxidation of DMSO. On the graph there are five reduction peaks or shoulders and five corresponding oxidation peaks or shoulders. There are two central oxidation–reduction regions between about −0.400 V and +0.200 V, near the initial open-circuit potential of +0.071 V.

Anodic of these are two oxidation–reduction regions around 0.400–0.800 V due to products of the initial reduction of **2**. They are not present if the electrode is initialy oxidized. They are not present if the electrode is initially reduced but at a rotating electrode; reduction products will be removed and their oxidation cannot take place.

At −1.200 V to −0.400 V there is a reduction–oxidation region cathodic of the two central regions. Voltammograms obtained for solutions not containing **2** indicate that these peaks are due to products formed from the slight oxidation and reduction of solvent at the edges of the potential range.

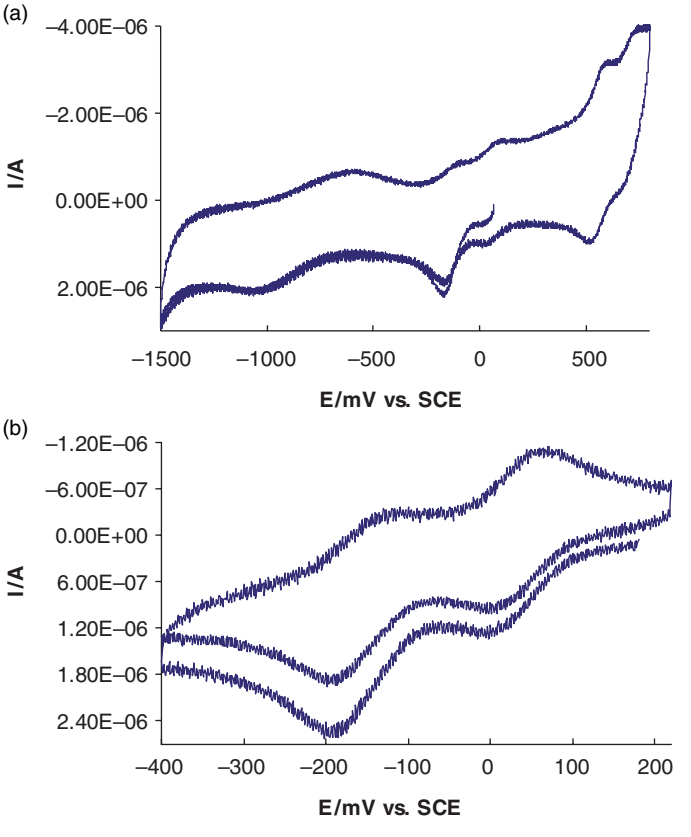

Figure 3. (a) Optimized structure of *mer*-[$RuCl_3$(DMSO-S)(DMSO-O)(py)] **2** in gas phase in which one DMSO is sulfur bonded and another via oxygen as in actual molecule in the crystal to ruthenium(III). (b) Optimized structure of *mer*-[$RuCl_3$(DMSO-S)(DMSO-O)(py)] **2** in gas phase in which sulfur and oxygen bonded to ruthenium(III) is switched compared to (a).

The two central oxidation–reduction regions are characteristic of **2**. Cyclic voltammetry was carried out with shorter sweeps that included only these two regions (figure 3). The voltammogram in figure 3 is characteristic of a reversible two-step system [17]. Peak separations in individual sweeps are about 200 mV but uncertainty in baselines prevents quantitative measurement of peak currents. The cathodic/anodic pair of peaks centered around 0.04 V is due to the Ru(III)/Ru(II) redox couple. The difference in potential between these two peaks (ΔE_p) ranges from 61 to 66 mV at sweep rates of 100–1003 mV s^{-1} and increases to 74 mV at 1505 mV s^{-1} and 96 mV at 3011 mV s^{-1}. The intermediate potential of these peaks ranged from 0.029 to 0.040 V with an average of 0.036 V. The close proximity of the two oxidation–reduction regions prevented full implementation of semi-derivative analysis [18], but the redox potential approximated as the average of the intermediate of the anodic and cathodic peak potentials on the semi-derivative graphs was 0.036 V.

The cathodic/anodic pair of peaks centered around −0.16 V is due to the Ru(II)/Ru(I) redox couple. For these two peaks, ΔE_p ranges from 61 to 64 mV at sweep rates of 200–1003 mV s^{-1} and increases to 84 mV at 1505 mV s^{-1} and 106 mV at 3011 mV s^{-1}. The intermediate potential of these peaks ranged from −0.161 to −0.167 V with an average of −0.163 V. Semi-derivative analyses gives an approximate redox potential of −0.162 V.

The correlation of Lever [19] predicts an approximate potential of 0.23 V for the Ru(III)/Ru(II) couple, at some variance with the value found here. Lever points out that DMSO is poorly behaved ligand for correlation. This may be a consequence of variable S or O coordinate bonding, which was not considered by Lever.

Supplementary material

Complete crystallographic data tables for **2** have been deposited with Cambridge Crystallographic Database in CIF format. Copies of this information may be obtained free of charge from the Director, CCDC, 12 Union Road, Cambridge, CB21EZ, UK (Fax: +44-1223-336-033; Email: deposit@ccdc.cam.ac.uk; www: http://www.ccdc.cam.ac.uk). CCDC deposit number is CCDC 697452.

Acknowledgments

Financial support provided by the Research Corporation (Cottrell College Science Award, #CC 6234) and the Louisiana Board of Regents Support Fund (to RSS) is greatly appreciated. The purchase of the diffractometer was made possible by Grant No. LEQSF (1999–2000)-ESH-TR-13, (to FRF) administered by the Louisiana Board of Regents.

References

[1] (a) S.-I. Murahashi, H. Takaya, T. Naota. *Pure Appl. Chem.*, **74**, 19 (2002); (b) T. Naota, H. Takaya, S.-I. Murahashi. *Chem. Rev.*, **98**, 2599 (1998); (c) D.P. Riley, J.D. Oliver. *Inorg. Chem.*, **25**, 1825 (1996); (d) M. Rodriguez, I. Romero, A. Llobet, A. Deronzier, M. Biner, T. Parella, H. Soteckli-Evans. *Inorg. Chem.*, **40**, 4150 (2001); (e) C.W. Chronister, R.A. Binstead, J. Ni, T.J. Meyer. *Inorg. Chem.*, **36**, 3814 (1997); (f) U.J. Jauregui-Haza, M. Dessoudeix, P. Kalck, A.M. Wilhelm, H. Delmas. *Catal. Today*, **66**, 297 (2001).

[2] (a) R. Ballardini, V. Balzani, A. Credi, M.T. Ganolfi, M. Venturi. *Int. J. Photoenergy*, **3**, 63 (2001); (b) P.R. Ashton, R. Ballardini, V. Balzani, A. Credi, K.R.. Dress, E. Ishow, C.J. Kleverlaan, O. Kocian, J.A. Preece, N. Spenser, J.F. Stoddart, M. Venturi, S. Wenger. *Chem. Eur. J.*, **6**, 3558 (2000); (c) E. Baranoff, J.-P. Collin, J. Furusho, Y. Furusho, A.-C. Laemmel, J.-P. Sauvage. *Inorg. Chem.*, **41**, 1215 (2002).
[3] M. Iwamoto, E. Alessio, L.G. Marzilli. *Inorg. Chem.*, **35**, 2384 (1996).
[4] (a) A. Tomita, M. Sano. *Chem. Lett.*, **25**, 981 (1996); (b) M. Sano, H. Taube. *J. Am. Chem. Soc.*, **113**, 2327 (1991); (c) A. Tomita, M. Sano. *Inorg. Chem.*, **39**, 200 (2000); (d) M. Sano, H. Sago, A. Tomita. *Bull. Chem. Soc. Jpn.*, **69**, 977 (1996); (e) M. Sano. *Inorg. Chem.*, **33**, 705 (1994).
[5] (a) S.C. Weatherly, I.V. Yang, H.H. Thorp. *J. Am. Chem. Soc.*, **123**, 1236 (2001); (b) S.O. Kelly, J.K. Barton. *Science*, **238**, 375 (1999); (c) D.B. Hall, R.E. Holmlin, J.K. Barton. *Nature*, **384**, 731 (1996); (d) C.J. Burrows, J.G. Muller. *Chem. Rev.*, **98**, 1109 (1998); (e) G.B. Schuster. *Acc. Chem. Res.*, **33**, 253 (2000).
[6] E. Alessio, G. Mestroni, A. Bergamo, G. Sava. *Met. Ions Biol. Syst.*, **42**, 323 (2004).
[7] I. Kostova. *Curr. Med. Chem.*, **13**, 1085 (2006).
[8] (a) D. Akbayeva, L. Gonsalvi, W. Oberhauser, M. Peruzzini, F. Vizza, P. Brugeller, A. Romerosa, G. Sava, A. Bergamo. *Chem. Commun.*, 264 (2003); (b) G. Pintus, B. Tadolini, A.M. Posadino, B. Sanna, M. Debidda, F. Bennardini, G. Sava, C. Ventura. *Eur. J. Biochem.*, **269**, 5861 (2002); (c) F. Frausin, M. Cocchietto, A. Bergamo, V. Scarcia, A. Furlani, G. Sava. *Cancer Chemother. Pharmacol.*, **50**, 405 (2002); (d) S. Zorzet, A. Bergamo, M. Cocchietto, A. Sorc, B. Gava, E. Alessio, E. Iengo, G. Sava. *J. Pharmacol. Exp. Ther.*, **295**, 927 (2000); (e) R.E. Morris, R.E. Aird, P. del Socorro Murdoch, H. Chen, J. Cummings, N.D. Hughes, S. Parsons, A. Parkin, G. Boyd, D.I. Jodrell, P.J. Sadler. *J. Med. Chem.*, **44**, 3616 (2001); (f) F. Wang, H. Chen, J.A. Parkinson, P. del Socorro Murdoch, P.J. Sadler. *Inorg. Chem.*, **41**, 4509 (2002); (g) H. Chen, J.A. Parkinson, S. Parsons, R.A. Coxall, R.O. Gould, P.J. Sadler. *J. Am. Chem. Soc.*, **124**, 3064 (2002); (h) E. Gallori, C. Vettori, E. Alessio, F. Gonzalez Vilchez, R. Vilaplana, P. Orioli, A. Casini, L. Messori. *Arch. Biochem. Biophys.*, **376**, 156 (2000); (i) A. Küng, T. Pieper, B.K. Keppler. *J. Chromatogr. B: Biomed. Sci. Appl.*, **759**, 81 (2001); (j) A. Abufarag, J. Reedijk. *J. Inorg. Biochem.*, **59**, 137 (1995); (k) O.M.N. Dhubhghaill, W.R. Hagen, B.K. Keppler, K.-G. Lipponer, P.J. Sadler. *J. Chem. Soc., Dalton Trans.*, 3305 (1994); (l) M. Hartmann, K.-G. Lipponer, B.K. Keppler. *Inorg. Chim. Acta*, **267**, 137 (1998); (m) M.J. Clarke, F. Zhu, D.R. Frasca. *Chem. Rev.*, **99**, 2511 (1999); (n) D. Frasca, M.J. Clarke. *J. Am. Chem. Soc.*, **121**, 8523 (1999).
[9] S. Mylonas, A. Valavanidis, K. Dimitropoulus, M. Polissiouv, A.S. Tsiftsoglov, I.S. Vizirianakis. *Inorg. Biochem.*, **34**, 265 (1988).
[10] E. Alessio, G. Balducci, M. Calligaris, G. Costa, W.M. Attia, G. Mestroni. *Inorg. Chem.*, **30**, 609 (1991).
[11] E. Alessio, G. Balducci, A. Lutman, G. Mestroni, M. Calligaris, W.M. Attia. *Inorg. Chim. Acta*, **203**, 205 (1993).
[12] R.S. Srivastava, F. Fronczek, N.R. Tarver, R.S. Perkins. *Polyhedron*, **26**, 5389 (2007).
[13] M.J. Frisch, G.W. Trucks, H.B. Schlegel, G.E. Scuseria, M.A. Robb, J.R. Cheeseman, J.A. Montgomery Jr, T. Vreven, K.N. Kudin, J.C. Burant, J.M. Millam, S.S. Iyengar, J. Tomasi, V. Barone, B. Mennucci, M. Cossi, G. Scalmani, N. Rega, G.A. Petersson, H. Nakatsuji, M. Hada, M. Ehara, K. Toyota, R. Fukuda, J. Hasegawa, M. Ishida, T. Nakajima, Y. Honda, O. Kitao, H. Nakai, M. Klene, X. Li, J.E. Knox, H.P. Hratchian, J.B. Cross, C. Adamo, J. Jaramillo, R. Gomperts, R.E. Stratmann, O. Yazyev, A.J. Austin, R. Cammi, C. Pomelli, J.W. Ochterski, P.Y. Ayala, K. Morokuma, G.A. Voth, P. Salvador, J.J. Dannenberg, V.G. Zakrzewski, S. Dapprich, A.D. Daniels, M.C. Strain, O. Farkas, D.K. Malick, A.D. Rabuck, K. Raghavachari, J.B. Foresman, J.V. Ortiz, Q. Cui, A.G. Baboul, S. Clifford, J. Cioslowski, B.B. Stefanov, G. Liu, A. Liashenko, P. Piskorz, I. Komaromi, R.L. Martin, D.J. Fox, T. Keith, M.A. Al-Laham, C.Y. Peng, A. Nanayakkara, M. Challacombe, P.M.W. Gill, B. Johnson, W. Chen, M.W. Wong, C. Gonzalez, J.A. Pople. Gaussian, Inc., Pittsburgh, PA (2003).
[14] J. Jaswal, S.J. Rettig, B.R. James. *Can. J. Chem.*, **68**, 1808 (1990).
[15] (a) E.C. Constable. *Adv. Inorg. Chem.*, **34**, 1 (1989); (b) E.C. Constable, C.E. Housecroft, M. Neuberger, I. Poleschak, M. Zehnder. *Polyhedron*, **22**, 93 (2003).
[16] (a) M. Calligaris, N. Presciani-Pahor, R.S. Srivastava. *Acta Crystallogr.*, **C49**, 448 (1993); (b) M. Calligaris. *Coord. Chem. Rev.*, **248**, 351 (2004); (c) M. Calligaris, O. Carugo. *Coord. Chem. Rev.*, **153**, 83 (1996).
[17] D.S. Polcyn, I. Shain. *Anal. Chem.*, **38**, 370 (1966).
[18] P. Dalrymple-Alford, M. Goto, K.B. Oldham. *J. Electroanal. Chem.*, **85**, 1 (1977).
[19] A.B.P. Lever. *Inorg. Chem.*, **29**, 1271 (1990).